X–OH and O–H⋯O Bond Lengths in Protonated Oxoanions

By Giovanni Ferraris and Gabriella Ivaldi

Istituto di Mineralogia, Cristallografia e Geochimica 'G. Spezia' dell' Università, Via S. Massimo 22, 10123 Torino, Italy

Abstract

A survey of the X–OH bonds in protonated oxoanions (X = B, C, N, Si, P, S, As, Se and I; coordination numbers 3 and/or 4) and of the hydrogen bonds donated by the corresponding OH shows the following trends. (i) For a given oxoanion, X–OH tends to increase in length with the distance O⋯O of the hydrogen bond; in particular, the overall average value of O⋯O for each X is inversely correlated with the natural logarithm of Pauling's bond strength p which is donated by X to OH. (ii) The average length of X–OH tends to decrease from mono- to triprotonated anions with the same X.

Introduction

Variously defined bond strengths (Baur, 1970; Brown & Shannon, 1973; Donnay & Allmann, 1970; Ferraris & Catti, 1973; Pyatenko, 1973), orbitals (Cruickshank, 1961), bond-overlap populations (*e.g.* Gibbs, Hamil, Louisnathan, Bartell & Yow, 1972), coordination number (Baur, 1978), mean electronegativity of the cations in the structure (Shannon & Calvo, 1973) and distortion of the coordination polyhedron (Baur, 1974) are some of the parameters which, singularly or jointly, have been correlated with the variations of individual or mean bond lengths in oxoanions. Less attention has, instead, been paid to the connections among two or more bonds involving the same atom; exceptions are the hydrogen bond in crystalline hydrates (Chiari & Ferraris, 1982; Ferraris & Franchini-Angela, 1972; Ichikawa, 1978), correlations of C–O *vs* O–H in hydrogen-bonded carboxyls (Ichikawa, 1979) and of S–OH *vs* O–H⋯O in sulphates (Catti, Ferraris & Ivaldi, 1979). The latter results are here extended to the X–OH bonds of protonated oxoanions where X = B, C, N, Si, P, S, As, Se, and I and the coordination number is 3 and/or 4.

Results

Structural data for a large number of compounds containing protonated oxoanions have been published, particularly for phosphates because of their important role in inorganic, organic and biological chemistry. Owing to disorder involving the proton, symmetry ambiguities and poor accuracy, about half* the crystal structures retrieved have been excluded from the present research, whose results are, anyway, essentially qualitative. The outcome of the survey is summarized in Tables 1 and 2. Standard deviations σ of the average values are also given, but their meaning is doubtful because they are obtained with the assumption of a normal distribution of the values. In fact, in addition to the smallness of some of the samples, the distributions (not reported) are usually quite asymmetric and sometimes show more than one maximum, *e.g.* one for very short hydrogen bonds and another for the other cases.

Scatter diagrams of X–OH *vs* the O⋯O distance in the donated hydrogen bond are shown in Fig. 1; for phosphates, arsenates and selenites there are enough neutron-diffraction results to justify diagrams of X–OH *vs* O–H and H⋯O as well (Fig. 2). In the figures distinction has been made for differently protonated anions. A diagram for nitrates is not reported because only three values are available (Table 1). Fig. 3 shows the variation of the mean overall distance $(O⋯O)_{av}$ for the hydrogen bonds donated by each type of oxoanion against the natural logarithm of Pauling's bond strength p (in valence units, v.u.) which each O receives from X. The bridge O of the P_2O_7 group has been assumed to receive 2 v.u., one from each P; the remaining 4 v.u. of each P have been distributed among the other oxygens ($\frac{4}{3}$ v.u. each).

The scattering of the experimental points would justify analytical correlations in only a few cases, as shown by the correlation coefficients R given in Tables 1 and 2. Anyway, in order to stress the trends which will be discussed below, least-squares-fitted straight lines are reported in Figs. 1 and 2 with the exceptions of borates, selenites and selenates which for the following and, maybe, other reasons show no

---

Table 1. *Average length* (Å) *of the bond X*–OH [(*X*–OH)av] *and of its donated hydrogen bond* [(O···O)av] *in tri- and tetracoordinated oxoanions where X is the coordinating atom*; σ_{X-OH} *and* $\sigma_{O···O}$ *are the corresponding standard deviations*

For each *X* the Pauling bond strength *p* (v.u.) donated to each coordinated O is reported; *R* and *S* are the correlation coefficient and the slope, respectively, of the corresponding least-squares straight line shown in Fig. 1.

Anion	No. of bonds	(O···O)av	$\sigma_{O···O}$	(*X*–OH)av	σ_{X-OH}	*p*	*R*	*S*
$(HBO_4)^{4-}$	19	2·790 Å	0·09 Å	1·465 Å	0·02 Å			
$(H_2BO_4)^{3-}$	17	2·847	0·12	1·481	0·02			
$(H_3BO_4)^{2-}$	7	2·817	0·06	1·485	0·02			
All	43	2·817	0·10	1·475	0·02	$\frac{3}{4}$		
$(HBO_3)^{2-}$	34	2·736	0·08	1·372	0·01			
(H_3BO_3)	12	2·717	0·02	1·364	0·01			
All	46	2·731	0·07	1·370	0·01	1		
$(HSiO_4)^{3-}$	6	2·628	0·15	1·685	0·01			
$(H_2SiO_4)^{2-}$	7	2·743	0·10	1·673	0·02			
All	13	2·690	0·13	1·678	0·02	1	0·32	0·05
$(HAsO_4)^{2-}$	36	2·610	0·13	1·731	0·02		0·43	0·08
$(H_2AsO_4)^{-}$	37	2·638	0·13	1·709	0·02		0·66	0·12
(H_3AsO_4)	3	2·651	0·15	1·697	0·01			
All	76	2·625	0·13	1·719	0·02	$\frac{5}{4}$		
$(HPO_4)^{2-}$	44	2·597	0·10	1·581	0·02		0·55	0·12
$(H_2PO_4)^{-}$	135	2·574	0·08	1·564	0·02		0·60	0·13
(H_3PO_4)	30	2·578	0·08	1·544	0·01		0·81	0·14
All	209	2·580	0·08	1·565	0·02	$\frac{5}{4}$		
$(HCO_3)^{3-}$	8	2·560	0·07	1·331	0·02	$\frac{4}{3}$	0·96	0·19
$(HP_2O_7)^{3-}$	6	2·513	0·04	1·564	0·02			
$(H_2P_2O_7)^{2-}$	12	2·551	0·05	1·554	0·02			
$(H_3P_2O_7)^{-}$	6	2·507	0·11	1·538	0·01			
All	24	2·530	0·07	1·552	0·02	$\frac{5}{4}$	0·54	0·17
$(HSeO_3)^{-}$	18	2·639	0·09	1·759	0·02			
(H_2SeO_3)	35	2·572	0·04	1·736	0·02			
All	53	2·595	0·06	1·744	0·02	$\frac{4}{3}$		
$(HSO_4)^{-}$	30	2·569	0·07	1·555	0·02			
(H_2SO_4)	4	2·595	0·06	1·530	0·02			
All	34	2·572	0·07	1·552	0·02	$\frac{6}{4}$	0·59	0·20
$(HSeO_4)^{-}$	11	2·565	0·10	1·710	0·02			
(H_2SeO_4)	1	2·459		1·730				
All	12	2·556	0·10	1·712	0·02	$\frac{6}{4}$		
(HNO_3)	3	2·535	0·07	1·339	0·004	$\frac{5}{3}$		
(HIO_3)	12	2·653	0·07	1·899	0·03	$\frac{5}{3}$	0·60	0·30

Table 2. *Average lengths* (Å) *of the bond X*–OH [(*X*–OH)av], *of* O–H [(O–H)av] *and of the corresponding* H···O [(H···O)av] *distance in the donated hydrogen bond*; σ_{X-OH}, σ_{O-H} *and* $\sigma_{H···O}$ *are the corresponding standard deviations*

$R_{H···O}$ and R_{O-H} are the correlation coefficients of the least-squares straight lines shown in Fig. 2 for *X*–OH *vs* H···O and O–H, respectively; $S_{H···O}$ and S_{O-H} are the corresponding slopes. Data are from structures studied by neutron diffraction only.

Anion	No. of bonds	(H···O)av	$\sigma_{H···O}$	(O–H)av	σ_{O-H}	(*X*–OH)av	σ_{X-OH}	$R_{H···O}$	R_{O-H}	$S_{H···O}$	S_{O-H}
$(HPO_4)^{2-}$	11	1·486 Å	0·18 Å	1·094 Å	0·09 Å	1·573 Å	0·02 Å	0·55	−0·78	0·07	−0·16
$(H_2PO_4)^{-}$	37	1·535	0·15	1·038	0·07	1·565	0·02	0·76	−0·75	0·09	−0·18
(H_3PO_4)	21	1·559	0·14	1·023	0·07	1·543	0·01	0·85	−0·80	0·08	−0·18
All	69	1·534	0·16	1·042	0·07	1·560	0·02				
All arsenates	14	1·583	0·22	1·053	0·09	1·718	0·03	0·79	−0·84	0·09	−0·23
All selenites	30	1·550	0·12	1·049	0·08	1·742	0·02	0·67	−0·64	0·11	−0·15

trends at all. Borates contain several types of complex anions for which separate statistics should be applied (*cf.* phosphates and pyrophosphates). Besides, each O receives from boron a *p* value of $\frac{3}{4}$ and 1 v.u. in tetrahedral and triangular coordinations, respectively; therefore, OH could not be the donor of a hydrogen bond, unless it takes further bond strength from coordination bonds. In such a context, trends which can be detected for other protonated oxoanions, where OH is usually bonded only to *X* and to the acceptor of its hydrogen bond, are concealed by the influence of other types of bonds. Cor-
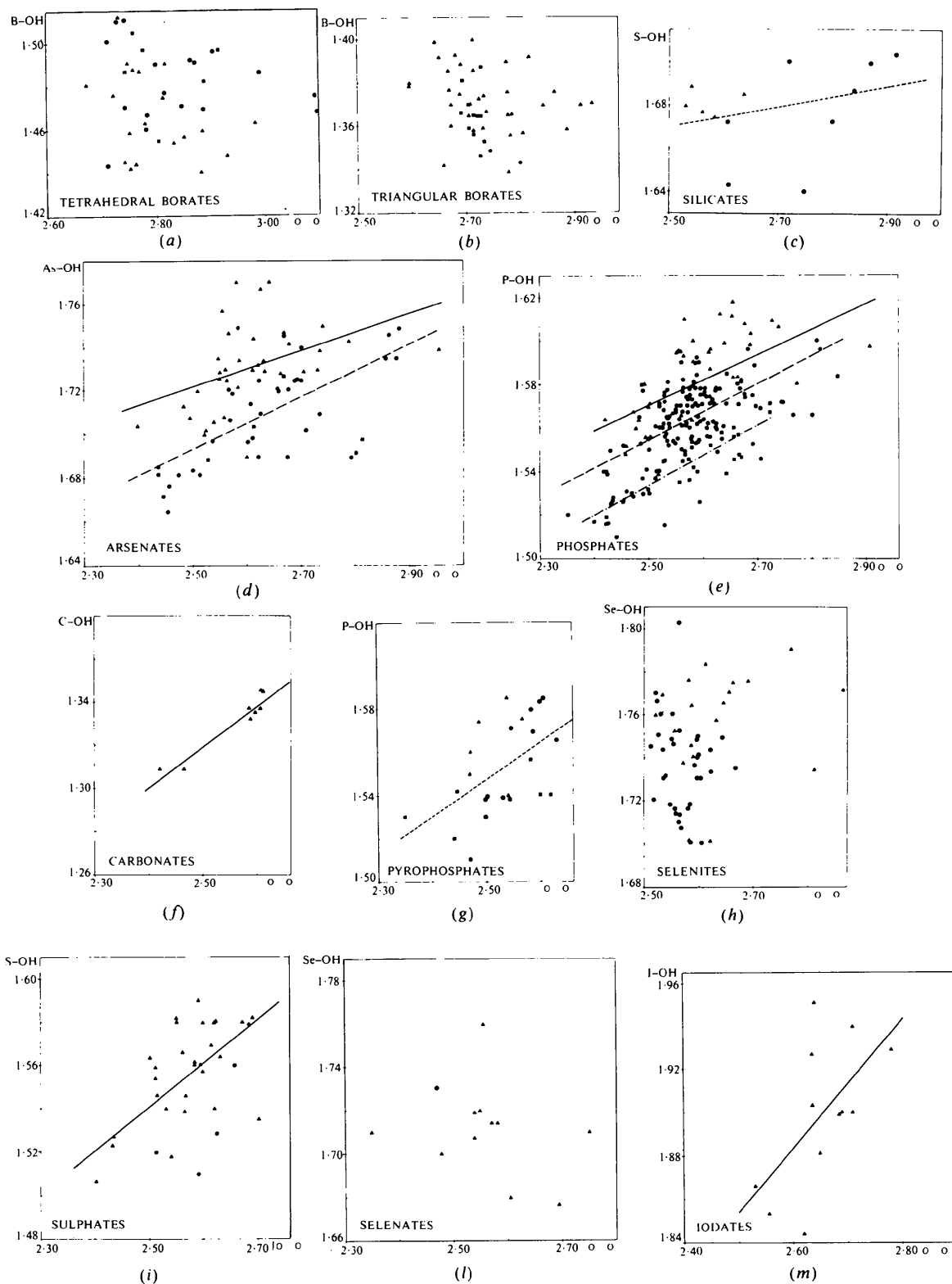
Fig. 1. Scatter diagrams for X–OH vs O$\cdots$O (Å). Triangles, circles and squares represent experimental values for mono-, bi- and triprotonated oxoanions, respectively. In the same order, they are in some cases fitted by full, dashed and dotted-dashed lines; short-dashed lines in (c) and (g) fit all points.

roboration of the influence of a value of $p \leqq 1$ comes from the diagram of Si [Fig. 1(c)] which shows the lowest of the reported correlation factors R (Table 1). A cause for the lack of correlation for the values of selenites [Fig. 1(h)] and selenates [Fig. 1(l)] could be the presence of structures with undetected disorder of the proton; in fact, these compounds are often studied structurally in view of their ferroelectric properties. On the other hand, good correlations are obtained with the more reliable (for the proton position) values from selenites studied by neutron diffraction [Figs. 2(e) and 2(f)].

Discussion

As recalled in the *Introduction*, the lengths of individual bonds are, to different extents, functions of several parameters; therefore, only qualitative bilateral correlations must be expected which, anyhow, can be useful to point out trends. As shown by the diagrams of Fig. 2 and the correlation coefficients R (Table 2), O–H and H···O bond lengths would be better indicators of the connections between X–OH and the hydrogen bond; unfortunately, enough reliable bonds involving H are available for only three types of oxoanions.
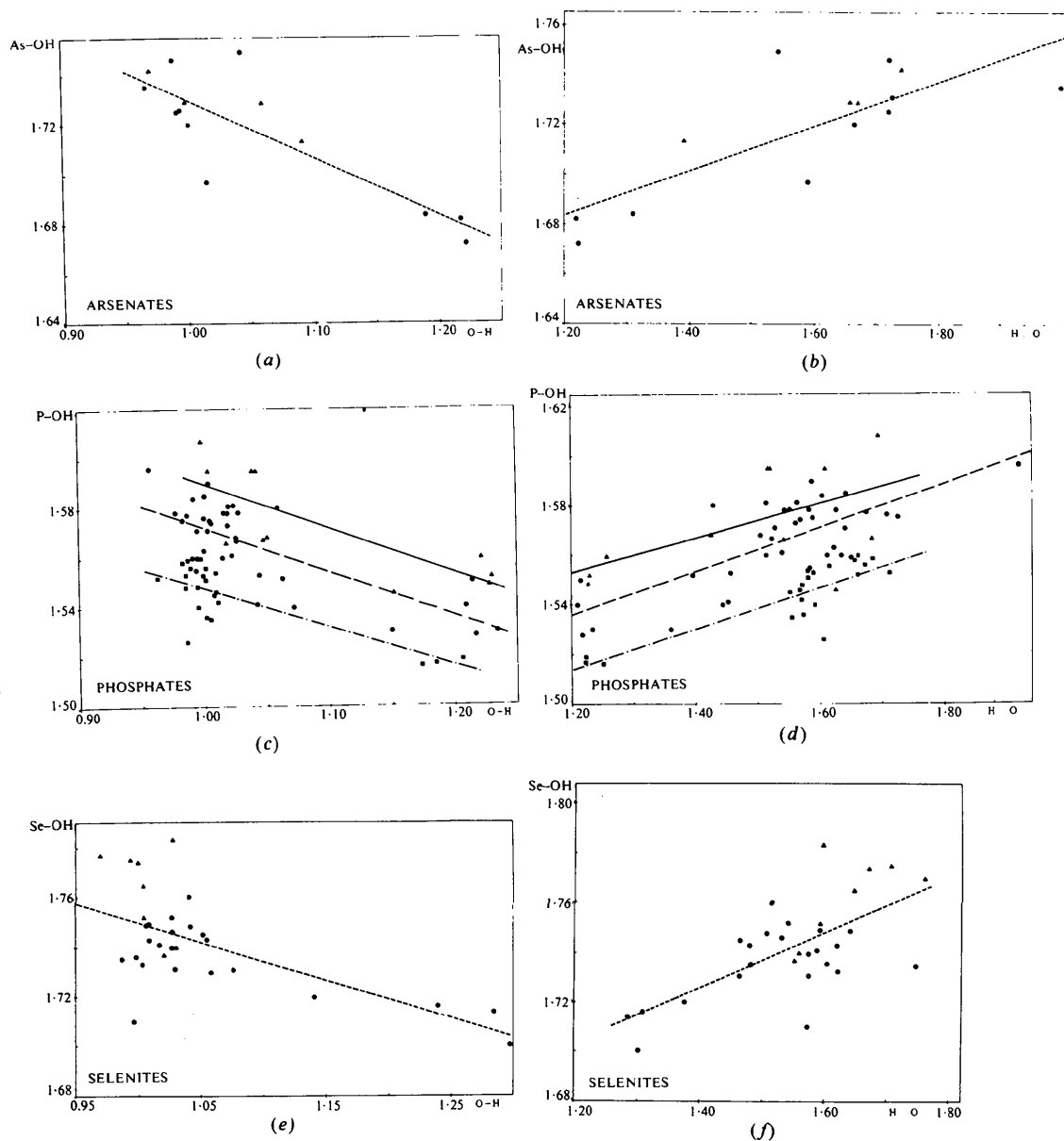

Fig. 2. Scatter diagrams for X–OH *vs* O–H and H···O (Å); experimental values from neutron-diffraction structures only. Symbols as in Fig. 1.

Average bond lengths

In spite of the spread of individual bond lengths in oxoanions and of the systematic differences between X–O and X–OH, a constancy of the average X–O (OH included) distance for all the bonds within each coordination polyhedron is well documented (Baur, 1970, 1974; Shannon & Prewitt, 1969) and only some second-order variations are known (Baur, 1978; Shannon & Calvo, 1973). In particular, no significant differences have been reported among $(X$–O$)_{av}$ of anions with the same X but different degree of protonation. Instead, at least for phosphates, separate average values for X–O and X–OH decrease from unprotonated $(X$–O only) to triprotonated anions (Baur, 1974). The present survey shows that such a behaviour is present in the majority of the oxoanions of Table 1, at least qualitatively; in fact, besides the reasons already pointed out, the smallness of several groups does not allow a satisfactory statistical treatment. Some understanding of the phenomenon can be attempted in terms of Pauling's bond strength p. Except for X = B and Si, the value of p received from X by each O is larger than 1 v.u.; therefore, the O of OH tends to withdraw from X to avoid overbonding with the consequent shortening of the X–O bonds to keep $(X$–O$)_{av}$ constant. The benefit of such a redistribution of bond strength diminishes, for individual X–OH bonds, with the increase of the number of protons in the same anion, also because the number of X–O (OH excluded) which can be shortened reduces.

A strong inverse correlation $(R = -0.95)$ is found between $(O \cdots O)_{av}$ and the natural logarithm of the corresponding p donated by X to OH (Fig. 3). In other words, the greater is the overbonding of the O of OH, the shorter tends to be the donated hydrogen bond in order to exchange a larger bond strength; $(O \cdots O)_{av}$ ranges from 2·817 Å for tetrahedral borates $(p = \frac{3}{4}$ v.u.) to 2·535 Å for nitrates $(p = \frac{5}{3}$ v.u.) (Table 1). The value for the group HIO_3, which is the worst as regards the correlation (Table 1), is not reported in Fig. 3 because the crystallochemical behaviour of three-coordinated iodine is peculiar in having, usually, a second three-atom coordination sphere. The use of bond-length-depending bond strengths, e.g. Brown & Shannon's (1973) values calculated for $(X$–O$)_{av}$, could discriminate between anions with the same X but different degree of protonation; a correlation has, in fact, been noticed but it is not presented here because of its strong non-linearity.

X–OH vs O–H$\cdots$O

The trend for X–OH to decrease in length with O$\cdots$O is general, with the exceptions pointed out for B and Se compounds (Fig. 1). The effect is due to the well documented attraction of the proton towards the acceptor O, which increases with the shortening of the O$\cdots$O distance: the consequent weakening of the O–H bond causes the donor O to approach X. The correlations of X–OH with O–H and H$\cdots$O, when available (Fig. 2, Table 2), show the trend better; in fact, the distance O$\cdots$O is only a surrogate representative of the characteristics of the hydrogen bond and its use surely overlooks such sources of errors as proton disorder, polyfurcated hydrogen bonds and influence of the O–H$\cdots$O angle.

The shorter is $(O \cdots O)_{av}$ the steeper are the least-squares straight lines of Fig. 1, as proved by the value S of their slopes (Table 1). In fact, owing to the non-linearity of the correlation between O$\cdots$O and the bond strength (Brown & Shannon, 1973; Brown, 1976), the same variation of O$\cdots$O requires a larger bond strength (larger variation of X–OH) for shorter hydrogen bonds.
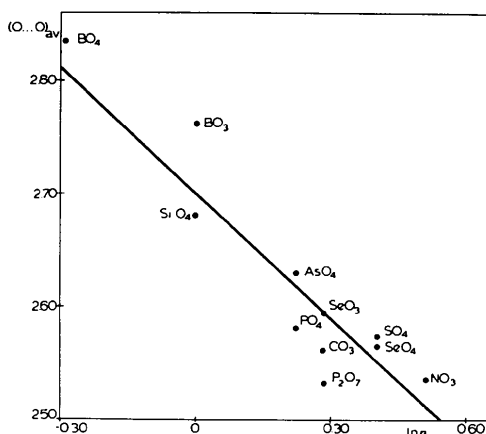
Fig. 3. Average O$\cdots$O distance (Å) for each type of oxoanion against the natural logarithm of Pauling's bond strength p. The equation of the regression straight line is $(O \cdots O)_{av} = -0.38 (11) \ln p + 2.70 (28)$ with a correlation coefficient $R = -0.95$.

References

BAUR, W. H. (1970). *Trans. Am. Crystallogr. Assoc.* **6**, 123–155.
BAUR, W. H. (1974). *Acta Cryst.* **B30**, 1195–1215.
BAUR, W. H. (1978). *Acta Cryst.* **B34**, 1751–1756.
BROWN, I. D. (1976). *Acta Cryst.* **A32**, 24–31.
BROWN, I. D. & SHANNON, R. D. (1973). *Acta Cryst.* **A29**, 266–282.
CATTI, M., FERRARIS, G. & IVALDI, G. (1979). *Acta Cryst.* **B35**, 525–529.
CHIARI, G. & FERRARIS, G. (1982). *Acta Cryst.* **B38**, 2331–2341.
CRUICKSHANK, D. W. J. (1961). *J. Chem. Soc.* pp. 5486–5504.
DONNAY, G. & ALLMANN, R. (1970). *Am. Mineral.* **55**, 1003–1015.

FERRARIS, G. & CATTI, M. (1973). *Acta Cryst.* B29, 2006–2009.
FERRARIS, G. & FRANCHINI-ANGELA, M. (1972). *Acta Cryst.* B28, 3572–3583.
GIBBS, G. V., HAMIL, M. M., LOUISNATHAN, S. J., BARTELL, L. S. & YOW, H. (1972). *Am. Mineral.* 57, 1578–1613.
ICHIKAWA, M. (1978). *Acta Cryst.* B34, 2074–2080.

ICHIKAWA, M. (1979). *Acta Cryst.* B35, 1300–1301.
PYATENKO, YU. A. (1973). *Sov. Phys. Crystallogr.* 17, 677–682.
SHANNON, R. D. & CALVO, C. (1973). *J. Solid State Chem.* 6, 538–549.
SHANNON, R. D. & PREWITT, C. T. (1969). *Acta Cryst.* B25, 925–946.

The Crystal Structures of Sodalite-Group Minerals

BY I. HASSAN* AND H. D. GRUNDY

Department of Geology, McMaster University, Hamilton, Ontario, Canada L8S 4M 1

Abstract

Sodalite, $Na_8(Al_6Si_6O_{24})Cl_2$, is cubic, $P\bar{4}3n$, $M_r = 969\cdot2$, $F(000) = 476$, $a = 8\cdot882(1)\text{Å}$, $D_x = 2\cdot30\text{ Mg m}^{-3}$, $Z = 1$, $R = 0\cdot017$ for 157 unique observed reflections measured on an automated four-circle X-ray diffractometer using Mo $K\alpha$ radiation. The 1:1 aluminosilicate framework is completely ordered. A geometrical sodalite model has been developed, which, when calibrated with the parameters from the refined structure, enables: (1) the accurate prediction of the atomic coordinates of all members of the sodalite-group minerals at both room and elevated temperatures; (2) the prediction of the chemical limits of structural stability of all such materials; (3) thermal-expansion data and substitution of interframework ions to be rationalized and predicted in terms of the rotation of the $(Al, Si)O_4$ tetrahedra.

Introduction

Minerals in the aluminosilicate sodalite group are characterized by an ordered framework of AlO_4 and SiO_4 tetrahedra. The cubic symmetry is the result of the close packing of interconnected sixfold rings of $(Al, Si)O_4$ tetrahedra. These six-membered rings are stacked parallel to {111} in an *ABCABC...* type of sequence. The structure is further characterized by $(Al, Si)O_4$ rings of four tetrahedra parallel to {100}. The overall linkage of $(Al, Si)O_4$ tetrahedra results in a cubo-octahedral cavity (Fig. 1). The six-membered rings form continuous channels that offer diffusion paths for interframework ions (Barrer & Vaughan, 1971).

The aluminosilicate framework of the sodalite-group minerals $(Al_6Si_6O_{24})^{6-}$ is isotypic with the framework of beryllosilicate $(Be_6Si_6O_{24})^{12-}$ (Pauling, 1930); borate $(B_{12}O_{24})^{12-}$ (Smith, García-Blanco & Rivoir, 1961); aluminate $(Al_{12}O_{24})^{12-}$ (see Depmeier, 1979); and the naturally occurring mineral tugtupite $(Na_8Al_2Be_2Si_8O_{24}Cl_2)$ (Danø, 1966). Ga- and Ge-substituted analogues of the aluminosilicate sodalites are also known (McLaughlan & Marshall, 1970). The sodalite cage is also used as a building unit in many zeolites (Meier, 1968) and several complicated structures, such as α-Mn, Sb_2Tl_7, tetrahedrite, *etc.*, can be described and related to that of sodalite (Nyman & Hyde, 1981). Within the sodalite cage a variety of cations and anions can be substituted. This paper examines in detail the aluminosilicate sodalites with interframework cations of the alkali group (Li^+, Na^+, K^+, Rb^+, Cs^+) and anions of the halide group (F^-, Cl^-, Br^-, I^-), and also the naturally occurring sulphatic sodalites nosean and hauyne.

Many of these sodalites have been synthesized by Henderson & Taylor (1977) and a computer model
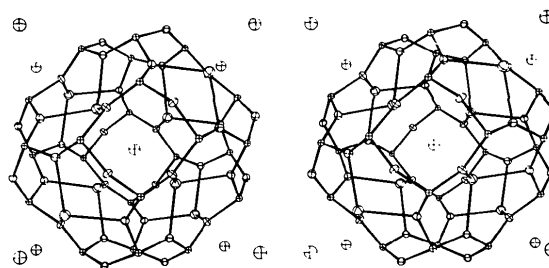

Fig. 1. Stereoscopic view of the sodalite structure showing the arrangement of AlO_4 and SiO_4 tetrahedra which gives the cubo-octahedral cavity. Small thermal ellipsoids represent Al or Si atoms, intermediate the framework oxygen, large the Na atoms in the vicinity of the six-membered rings and the isolated Cl atoms at the corners and centre of the cell.

* Present address: Earth and Planetary Sciences, Erindale Campus, University of Toronto, Ontario, Canada L5L 1C6.